In Vivo Powering of Pacemaker by Breathing-Driven Implanted Triboelectric Nanogenerator

Qiang Zheng, Bojing Shi, Fengru Fan, Xinxin Wang, Ling Yan, Weiwei Yuan, Sihong Wang, Hong Liu, Zhou Li, and Zhong Lin Wang**

A long-lasting power source is crucial for a sustainable operation of implanted medical devices.[1,2] Owing to the limited life-time,[3,4] battery powered medical devices usually required additional surgery once in a while to replace the drained battery, which is not only non-economical but also increases painful experience and risk for patients. Therefore, it is desirable to have in vivo medical devices self-powered by harvesting energy from biological systems to maintain the sustainable operation of the devices. Many investigations focus on energy-harvesting strategies in order to replace batteries.[5,6] Several methods to harvest energy from chemical, mechanical, electrical, and thermal processes in the human body has been demonstrated, such as using glucose oxidation, the electric potentials of the inner ear, mechanical movements of limbs, and the vibration of organs.[7–11] Among all these energies, small scale mechanical energy is one of the most abundant and popular energies in a living environment. Harvesting biomechanical energy in vitro and in vivo can provide a nearly lifetime power source to drive the micro-/nanosystems. Piezoelectric devices as a potential route for mechanical-to-electrical energy transduction has been fabricated recently and shown numerous advantages.[12–19] Some of these piezoelectric devices can be made of biocompatible materials, and this made them possible for in vivo applications.[16,20–22] The first demonstration of an in vivo mechanical energy driven piezoelectric nanogenerator was demonstrated by Wang's group in 2010,[23] and the device has also further developed recently.[24] However, the main limitation is that the output of the piezotronic nanogenerators was rather limited so that it is not powerful enough to directly drive most medical devices.

Dr. Q. Zheng,[+] B. Shi,[+] Dr. F. Fan,[+] Dr. X. Wang, Prof. H. Liu, Prof. Z. L. Wang
Beijing Institute of Nanoenergy and Nanosystems
Chinese Academy of Science
Beijing 100083, PR China
E-mail: zlwang@binn.cas.cn

L. Yan, W. Yuan, Dr. Z. Li
Key Laboratory for Biomechanics and Mechanobiology of Ministry of Education
School of Biological Science and Medical Engineering
Beihang University
Beijing 100191, PR China
E-mail: lizhou@buaa.edu.cn

Dr. S. Wang, Prof. Z. L. Wang
School of Materials Science and Engineering
Georgia Institute of Technology
Atlanta, GA 30332, USA

[+]These author contributed equally in this work

DOI: 10.1002/adma.201402064

Recently, triboelectric nanogenerator (TENG) has attracted much attention.[25–29] The mechanism of the TENG relies on a conjunction of triboelectrification and electrostatic induction. It has been systematically studied to drive hundreds of light emitting diodes (LEDs)[26,28] and charge a lithium-ion battery[30] for powering some small equipment. Recently, the TENG has been employed to collect energy from human motion under in vitro conditions,[31–33] such as walking, running or clapping.

However, the applications of TENG under in vivo are distinct from in vitro environments, which are more complicated and challenging. Some crucial problems need to be addressed. For example, the in vivo environment is filled with body fluid, which will significantly affect the output performance of TENG[34] if it leaks into the gap between the friction layers of TENG. Thus, careful packaging is needed using biocompatible and soft materials. Secondly, the size and thickness of TENG need to be strictly controlled for the available space inside that is usually very narrow and irregular in shape. Another problem we should notice is that the in vivo movement is so gentle and the amplitude is so small that our TENG must be sensitive enough to catch such small scale motion.

In this paper, in vivo biomechanical-energy harvesting using a TENG is demonstrated for the first time. An implantable triboelectric nanogenerator (iTENG) in a living rat has been developed to harvest energy from its periodic breathing. Then, the breathing generated energy was directly used to power a prototype pacemaker. This is a significant progress for fabricating self-powered implanted medical devices using TENG as a power source.

The fabrication of the iTENG was based on the design of a fully packaged structure (**Figure 1**a). Basically, a PDMS film with patterned pyramid arrays (100 μm in thickness) was first made by spin-coating pre-mixed PDMS elastomer and crosslinker on a patterned Si wafer. After curing thermally, a uniform PDMS film was peeled off the silicon wafer mold, and then placed on a thin Kapton substrate (30 μm) deposited with Au (50 nm) (Figure 1b). The flexibility of the thin PDMS and Kapton layer made it able to deform easily in response to the slight in vivo motion caused by the rat breathing (Figure 1e). Aluminum foil with nano-surface modification served as both the contact layer and electrode of the iTENG (Figure 1c). In the presence of a flexible PET spacer (400 μm) in between the contact layers, the patterned PDMS film can be fully enclosed, which is very important for protecting the inner structure from the invasion of the surrounding physical environment. Thin wires were fixed to the back of both electrodes by applying silver paste. Because of the presence of bio-fluid under in vivo working condition, the entire device was covered with a flexible

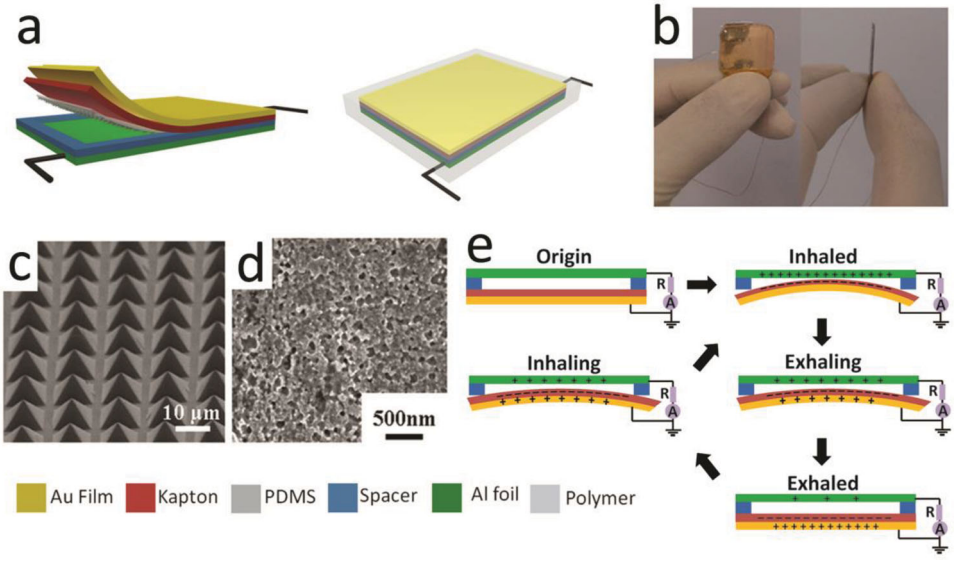

Figure 1. Structure and photograph of an implantable TENG. a) Schematic of the structure of the fabricated TENG. b) Photograph of the fabricated TENG. c) SEM image of PDMS film. d) SEM image of micro-nanostructure on an aluminum foil. e) Working principle of the iTENG.

polymer layer to isolate it from surrounding medium and to improve its robustness (see Supporting Information). Here, we use thin PDMS layer (ca. 50 μm) as the encapsulation material for its flexibility, leakproofness, biocompatibility and mild inflammatory reaction when implanted.[35]

The short-circuit current (I_{sc}) and open-circuit voltage (V_{oc}) were measured to examine the performance of the iTENG. As mentioned above, for fitting the special in vivo structure, the thickness and the size of the iTENG were carefully controlled; the overall size of the as fabricated iTENG was 1.2 cm × 1.2 cm. Since there was a spacer between these two fraction layers (Figure 1d), the contact area was only about 0.8 cm × 0.8 cm, which subsequently affected the output performance of iTENG. The output V_{oc} and I_{sc} are typically about 12 V and 0.25 μA, respectively (**Figure 2**a,b), the power density can still reach to 8.44 mW m^{-2} (Figure 2c,d).

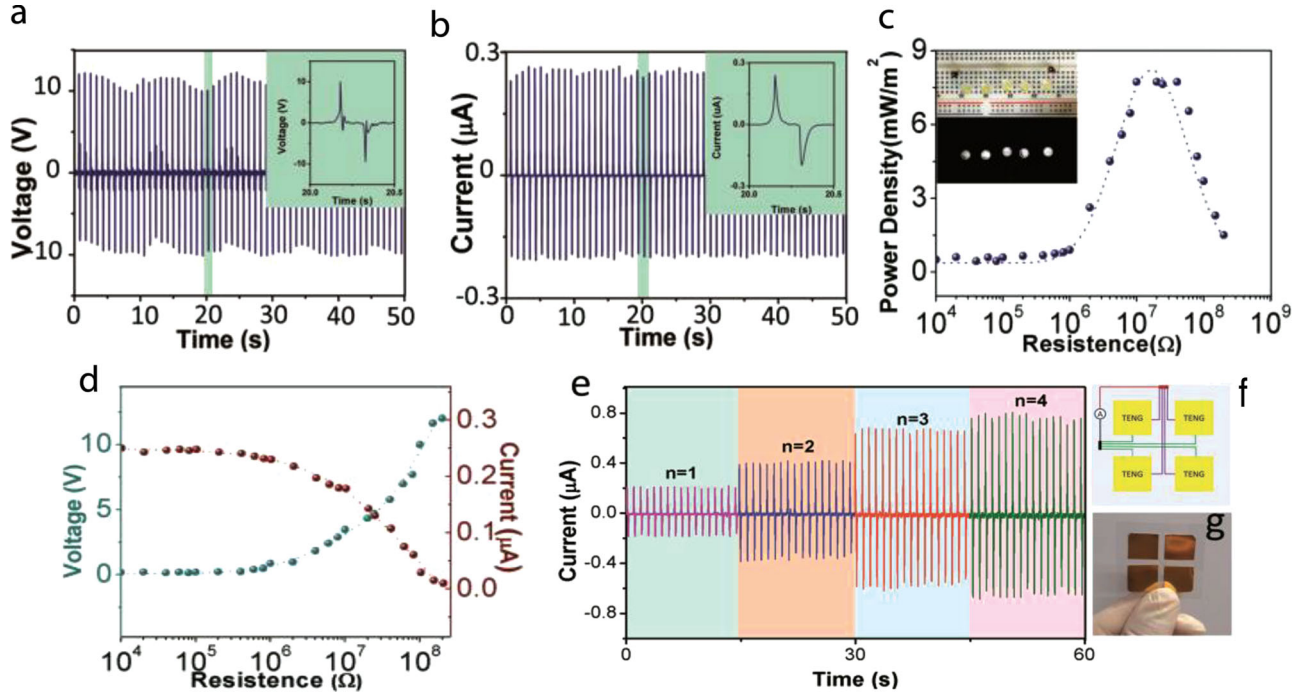

Figure 2. Output performance of an as fabricated implantable TENG. a) Typical voltage and b) current output of the iTENG. c,d) Dependence of output power density (the insert shows the lighting up of 5 white LEDs), output voltage, and output current of the iTENG as a function of the applied external load. e) The current output with different number of TENGs. f) Schematic diagram and g) photograph of the TENG array.

Adv. Mater. **2014**,
DOI: 10.1002/adma.201402064

In this experiment, the size of iTENG was strictly limited because we chose rats as the animal model to demonstrate the work system, which also limit the output of the iTENG. Actually, if used in the human body, size and structure could be re-designed for larger electrical output. Here, another group of experiments were carried out for illustrating the potential of output improvement of iTENG. We simply fabricated an array with different TENG number (1–4), the parallel connected 2×2 TENG array can generate a short-circuit current reaching to 0.8 μA, nearly 4 times that of a single TENG (Figure 2e–g). This illustrated that iTENG arrays or a bigger sized iTENG can be implanted in a human body for a higher output.

The animal experiment was based on the conversion of the mechanical deformation related to the periodic expansion and contraction of the thorax of a rat into electricity. Adult rats (Hsd: Sprague Dawley SD, male, 150–200 g) used for experiment were purchased from Peking University Health Science Center (PEUHSC), and our procedures in handling the animals was supervised by the Experimental Animal Ethics Committee of PEUHSC, which strictly followed the "Beijing Administration Rule of Laboratory Animals", and the national standards "Laboratory Animal Requirements of Environment and Housing Facilities (GB 14925–2001)". The anesthesia procedure of the rat started with the intake of isoflurane gas (1–3% in pure medical grade oxygen), followed by the injection of 1% sodium pentobarbital (intraperitoneal, 40 mg kg^{-1}) for anesthesia induction and maintenance, respectively. A tracheotomy was first performed, and a tracheal intubation was connected to a respirator, which provided artificial respiration and sustained life of the rat throughout the entire experiment. The left chest skin was incised for implanting the TENG. The pacemaker was placed in the chest (just below the collarbone);[36] implanting an iTENG near the site can harvest the mechanical energy from the periodic movement of the thorax and make it possible to integrate the iTENG and a pacemaker in the near future.

The iTENG was implanted under the left chest skin of the rat (**Figure 3**c,d). The inhalation and exhalation of the rat resulted in the alternative expansion and contraction of the thorax, which in turn produced deformation of the thin Kapton film, resulting in the periodical contacting and separating between the PDMS nanostructure and the Al foil, respectively. In this process, the electric potential induced by the contact electrification and electrostatic drove the electrons to flow back and forth through an external circuit in response to the respiratory motion (see Video S1 in the Supporting Information)

The short-circuit current and open-circuit voltage output from the iTENG were detected when the breathing of the rat was driven and controlled by the respirator at a constant rate of about 50 times per minute. When the measurement equipment was connected to the iTENG, a voltage/current pulse was produced during inhalation, immediately followed by a negative voltage/current pulse by exhalation. On average, the magnitude of the voltage and current signals was about 3.73 V and 0.14 μA, respectively (Figure 3a,b), which are lower than the output of former tests driven by mechanical simulation motor with higher strain rate and a larger degree of mechanical deformation. For powering most implantable devices or microchips, these outputs were still considerable.

There are about 50 "paired peak groups" in one minute, which is consistent with the breathing rate controlled by the respirator. Detailed information of the peaks was also inspected, which revealed that the first peak is slightly wider than the second one. This difference was attributed to the longer inhalation time than that of exhalation. Further more, the forced vital capacity (FVC) of the rat was also measured. In the typical FVC curve (Figure 3e, left), the ratio between the inspiratory reserve volume (IRV) and expiratory reserve volume (ERV) (the maximal volume of air that can be inhaled and exhaled from the end-inspiratory and end-expiratory position) was much similar with that between the peak values of the positive and negative current pulses

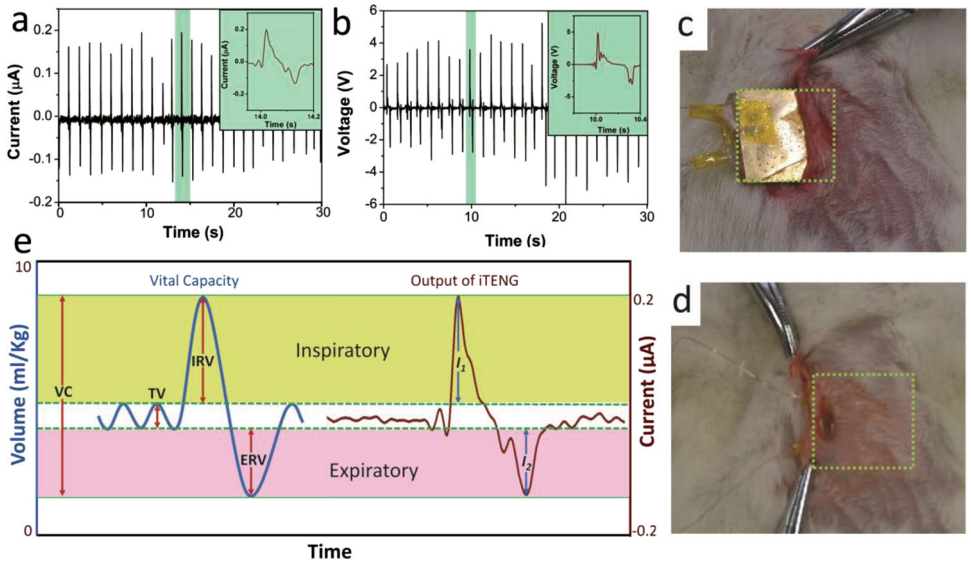

Figure 3. Energy harvesting from the breath of a living rat. a,b) An iTENG buried under the thoracic skin. c) Typical voltage and d) current output of TENG under in vivo conditions (from the set up in (b)). e) Correlation between the output of iTENG and respiratory movements (left: forced vital capacity curve; right: short-circuit current of the iTENG. VC: vital capacity; TV: tidal volume; IRV: inspiratory reserve volume; ERI: expiatory reserve volume).

(IRV/ERV = $|I_1|/|I_2|$), and more over, an obvious synchronism was also found by comparing the tendency of FVC curve and the short-circuit current curve (Figure 3e, right). These details further confirmed the working principle we proposed before.

Powering medical devices directly with the energy harvested by iTENG, and forming a self-powered system is the main objective of this work. In order to demonstrate the function of this self-powered system, we fabricated a prototype pacemaker with adjustable parameters (frequency, width, and voltage of the stimulation pulse) as a model (**Figure 4**a,b). Here, we designed the prototype based on a 555 timer IC. It outputs a continuous stream of rectangular pulses at a specified frequency. Resistors (R_1, R_2, R_3) and capacitor C_1 co-determined the output performance of this prototype. Resistor R_1 was connected between the supply voltage and the discharge pin (pin 7) and another resistor (R_2) was connected between the discharge pin (pin 7) and the trigger (pin 2) and threshold (pin 6) pins that shared a common node. In order to achieve a duty cycle less than 50%, we set up two diodes (D_1 and D_2) to make sure that the capacitor (C_1) can be charged approximately only through R_1, and discharged only through R_2. The capacitor C_2 connected between pin 5 and ground is to provide interference, and resistor R_3 is used to adjust the magnitude of the voltage of the output pulse (Figure 4b).

For this prototype, the high time from each pulse can be given by:

$$T_h = \ln(2) \cdot R_1 \cdot C_1 \quad (1)$$

And the low time from each pulse can be given by:

$$T_l = \ln(2) \cdot R_2 \cdot C_1 \quad (2)$$

So, the frequency (f) of the pulse stream depends on the values of T_h and T_l:

$$f = \frac{1}{T_h + T_l} = \frac{1}{\ln(2) \cdot C_1 \cdot (R_1 + R_2)} \quad (3)$$

The pulse duty cycle (q) also can be achieved by:

$$q = \frac{R_1}{R_1 + R_2} \quad (4)$$

Basically, in the self-powered system, the AC output from iTENG could be transformed to a pulse output in the same

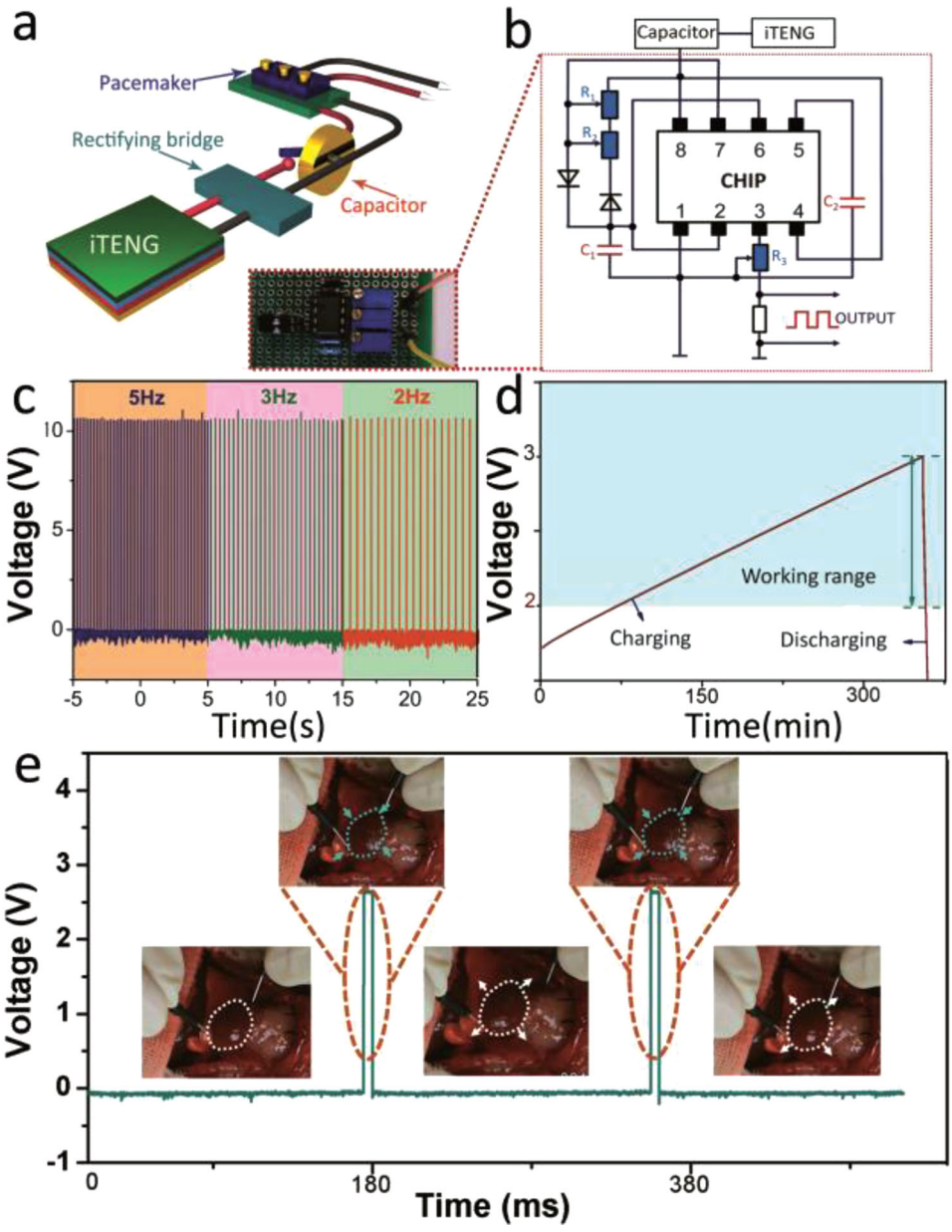

Figure 4. Scheme diagram of a self-powered prototype pacemaker. a) Structure and photograph of the self-powered pacemaker. b) Circuit diagram of prototype pacemaker ($R_1 \approx 0$–50 kΩ, $R_2 \approx 0$–200 kΩ, $R_3 \approx 0$–100 kΩ, $C_1 = 10$ μF, $C_2 = 0.01$ μF). c) Stimulation pulse with different frequencies generated by self-powered pacermaker. d) Charging curve of the capacitor by using implantable TENG. e) Stimulating the heart of the rat by self-powered pacemaker (insets: photographs of the heart beat of the rat regulated by self-powered pacemaker).

Adv. Mater. 2014,
DOI: 10.1002/adma.201402064

direction simply by using full-wave rectifying bridge and stored in a capacitor (Supporting Information, Figure S1). To our knowledge, the commercial pacemaker worked within a voltage range between 1.8–2.8 V, when the voltage decreased to a certain level (elected replacement index (ERI)), the device has to be replaced as soon as possible. In our experiment, the working range of the prototype was 2–3 V (Figure 4d), and therefore our charging and discharging tests were carried out in this range. The capacitor can be charged from 2 to 3 V within 275 min (for a total of 13750 breathing cycles) by the iTENG. The total charges (C_T) can be calculated based on Equation 5:

$$C_T = I_{TENG} \cdot W \cdot R_B \cdot T_C \quad (5)$$

Where I_{TENG} is the short-circuit current of iTENG, W is the pulse-width, R_B is the breath rate and T_C is the total charging time.

The output of a single stimulation pulse of the as-fabricated pacemaker prototype was about 25 μA (I_P), and the pulse width was set to 2 ms (t_P), which was comparable with the commercial pacemakers (Supporting Information, Figure S2). Based on these parameters, we can theoretically calculate that the energy generated during 5 breaths can stimulate a single pulse in iTENG (Equation 6). Then, the charged capacitor was applied to drive the pacemaker prototype and stimulation pulses with different frequency were successfully demonstrated (Figure 4c). Furthermore, we also used the iTENG powered pacemaker for regulating the heart rate of the rat (Figure 4e). Briefly, stimulation pulses with different working frequencies (2 Hz, 3 Hz and 5 Hz) generated by the pacemaker were applied to the heart, and apparently, the heart rate was regulated to synchronized with the frequency of the stimulation pulse (see Video S2, and S3 in the Supporting Information).

$$r = I_T t_T / I_p t_p \quad (6)$$

As we know, there are many kinds of implantable medical devices for applying in different implant sites. Assuring that our iTENG can work in more complicated bioenviroment is crucial for its wider application. **Figure 5** shows a re-designed iTENG that is set in between the diaphragm and the liver. A large size iTENG (3 cm × 2 cm) was applied, and the flexible thin Kapton layer was contacted with the surface of the diaphragm (Figure 5a,b). As the main muscle of respiration, its expansion and contraction can also drive the iTENG, and the larger size and greater degree of deformation generated a higher AC output (0.6 μA) (Figure 5c). During these experiments, a respirator was also used to serve as a life-sustaining device throughout the whole experiment, and a slower and deeper breath was used to get a more substantial deformation of diaphragm and avoid the influence of liver quiver (see Video S4 in the Supporting Information).

In summary, we have demonstrated an in vivo application of a TENG for harvesting biomechanical energy inside a living animal for the first time. The structure of the TENG was carefully designed; the shape and packaging were reconsidered to fit the implanted site and muscle movement of the animal thorax. This newly designed iTENG successfully converted the mechanical energy from the rat's normal breathing into electricity with a power density up to 8.44 mW m^{-2}. Moreover, the harvested energy from in vivo was demonstrated to drive an implantable medical device as a real application. The electricity from iTENG was stored in a capacitor and successfully drove a pacemaker prototype to regulate the heart rate of a rat. Our research shows a feasible approach to scavenge the biomechanical energy, such as heart beating, muscle stretching, blood flow, or even irregular vibration. This work presents a crucial step forward for lifetime implantable self-powered medical devices.

Supporting Information

Supporting Information is available from the Wiley Online Library or from the author.

Acknowledgements

The work was supported by the "Thousands Talents" program for pioneer researcher and his innovation team, Beijing Municipal Science & Technology Commission Z131100006013004, Beijing Nova Program

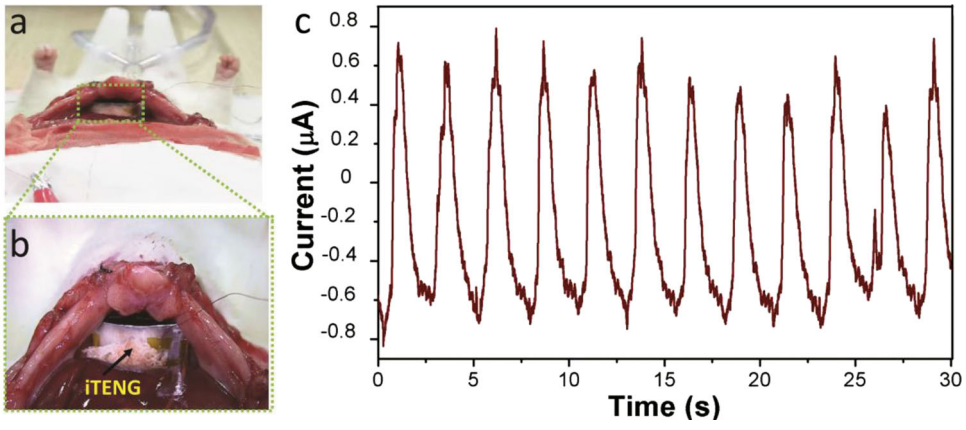

Figure 5. Energy harvesting from the diaphragmatic movement. a) An iTENG attached to a live rat's diaphragm (the dashed rectangular area shows the position of the iTENG). b) An enlarged picture of the iTENG. c) Typical current output of the iTENG that was attached to the rat's diaphragm.

Z121103002512019, Z131103000413116, the RFDP 20111102120038, NCET-12-0027, NSFC 31200702, Beijing Municipal NSF 713212.

Received: May 8, 2014
Revised: May 28, 2014
Published online:

[1] Medicines and Healthcare Products Regulatory Agency, MHRA http://www.mhra.gov.uk/Howweregulate/Devices/Complyingwithlegislation/ActiveImplantableMedicalDevicesDirective/index.htm, accessed **June 2014**.
[2] K. Lewandowski-Walker, U.S. Food and Drug Administration (FDA), http://www.fda.gov/downloads/medicaldevices/newsevents/workshopsconferences/ucm364417.pdf, accessed **June 2014**.
[3] V. S. Mallela, V. Ilankumaran, N. S. Rao, *Indian Pacing Electrophysiol. J.* **2004**, *4*, 201.
[4] F. W. Horlbeck, F. Mellert, J. Kreuz, G. Nickenig, J. O. Schwab, *J Cardiovasc. Electrophysiol.* **2012**, *23*, 1336.
[5] M. A. Karami, D. J. Inman, *Appl. Phys. Lett.* **2012**, 100.
[6] T. Starner, *IBM Syst. J.* **1996**, *35*, 618.
[7] L. Halamkova, J. Halamek, V. Bocharova, A. Szczupak, L. Alfonta, E. Katz, *J. Am. Chem. Soc.* **2012**, *134*, 5040.
[8] P. P. Mercier, A. C. Lysaght, S. Bandyopadhyay, A. P. Chandrakasan, K. M. Stankovic, *Nat. Biotechnol.* **2012**, *30*, 1240.
[9] L. S. Y. Wong, S. Hossain, A. Ta, J. Edvinsson, D. H. Rivas, H. Naas, *IEEE J. Solid-State Circuits* **2004**, *39*, 2446.
[10] S. R. Platt, S. Farritor, K. Garvin, H. Haider, *IEEE-Asme. T. Mech.* **2005**, *10*, 455.
[11] A. Zurbuchen, A. Pfenniger, A. Stahel, C. T. Stoeck, S. Vandenberghe, V. M. Koch, R. Vogel, *Ann. Biomed. Eng.* **2013**, *41*, 131.
[12] Z. L. Wang, J. H. Song, *Science* **2006**, *312*, 242.
[13] X. D. Wang, J. H. Song, J. Liu, Z. L. Wang, *Science* **2007**, *316*, 102.
[14] Z. L. Wang, *Adv. Mater.* **2012**, *24*, 4632.
[15] M. Y. Choi, D. Choi, M. J. Jin, I. Kim, S. H. Kim, J. Y. Choi, S. Y. Lee, J. M. Kim, S. W. Kim, *Adv. Mater.* **2009**, *21*, 2185.
[16] X. Chen, S. Y. Xu, N. Yao, Y. Shi, *Nano Lett.* **2010**, *10*, 2133.
[17] Y. Qi, M. C. McAlpine, *Energy Environ. Sci.* **2010**, *3*, 1275.
[18] K. I. Park, S. Xu, Y. Liu, G. T. Hwang, S. J. L. Kang, Z. L. Wang, K. J. Lee, *Nano Lett.* **2010**, *10*, 4939.
[19] G. T. Hwang, H. Park, J. H. Lee, S. Oh, K. I. Park, M. Byun, G. Ahn, C. K. Jeong, K. No, H. Kwon, S. G. Lee, B. Joung, K. J. Lee, *Adv. Mater.* **2014**.
[20] C. E. Chang, V. H. Tran, J. B. Wang, Y. K. Fuh, L. W. Lin, *Nano Lett.* **2010**, *10*, 726.
[21] J. Fang, X. G. Wang, T. Lin, *J. Mater. Chem.* **2011**, *21*, 11088.
[22] L. Persano, C. Dagdeviren, Y. W. Su, Y. H. Zhang, S. Girardo, D. Pisignano, Y. G. Huang, J. A. Rogers, *Nat. Commun.* **2013**, 4.
[23] Z. Li, G. Zhu, R. S. Yang, A. C. Wang, Z. L. Wang, *Adv. Mater.* **2010**, *22*, 2534.
[24] C. Dagdeviren, B. D. Yang, Y. W. Su, P. L. Tran, P. Joe, E. Anderson, J. Xia, V. Doraiswamy, B. Dehdashti, X. Feng, B. W. Lu, R. Poston, Z. Khalpey, R. Ghaffari, Y. G. Huang, M. J. Slepian, J. A. Rogers, *Proc. Natl. Acad. Sci. USA* **2014**, *111*, 1927.
[25] F. R. Fan, Z. Q. Tian, Z. L. Wang, *Nano Energy* **2012**, *1*, 328.
[26] G. Zhu, Z. H. Lin, Q. S. Jing, P. Bai, C. F. Pan, Y. Yang, Y. S. Zhou, Z. L. Wang, *Nano Lett.* **2013**, *13*, 847.
[27] S. H. Wang, L. Lin, Z. L. Wang, *Nano Lett.* **2012**, *12*, 6339.
[28] G. Zhu, J. Chen, Y. Liu, P. Bai, Y. S. Zhou, Q. S. Jing, C. F. Pan, Z. L. Wang, *Nano Lett.* **2013**, *13*, 2282.
[29] L. Lin, S. H. Wang, Y. N. Xie, Q. S. Jing, S. M. Niu, Y. F. Hu, Z. L. Wang, *Nano Lett.* **2013**, *13*, 2916.
[30] S. H. Wang, Z. H. Lin, S. M. Niu, L. Lin, Y. N. Xie, K. C. Pradel, Z. L. Wang, *ACS Nano* **2013**, *7*, 11263.
[31] H. L. Zhang, Y. Yang, T. C. Hou, Y. J. Su, C. G. Hu, Z. L. Wang, *Nano Energy* **2013**, *2*, 1019.
[32] T. C. Hou, Y. Yang, H. L. Zhang, J. Chen, L. J. Chen, Z. L. Wang, *Nano Energy* **2013**, *2*, 856.
[33] W. Q. Yang, J. Chen, G. Zhu, J. Yang, P. Bai, Y. J. Su, Q. S. Jing, X. Cao, Z. L. Wang, *ACS Nano* **2013**, *7*, 11317.
[34] H. L. Zhang, Y. Yang, Y. J. Su, J. Chen, C. G. Hu, Z. K. Wu, Y. Liu, C. P. Wong, Y. Bando, Z. L. Wang, *Nano Energy* **2013**, *2*, 693.
[35] M. C. Belanger, Y. Marois, *J. Biomed. Mater. Res.* **2001**, *58*, 467.
[36] Johns Hopkins Medicine Health Library, http://www.hopkinsmedicine.org/healthlibrary/test_procedures/cardiovascular/pacemaker_insertion_92,P07980/, accessed **June 2014**.